The investigation on the nonlinearity of plasticine-like magnetorheological material under oscillatory shear rheometry

Xinglong Gong (龚兴龙),[a] Yangguang Xu (许阳光), Shouhu Xuan (宣守虎),[b] Chaoyang Guo (郭朝阳), and Luhang Zong (宗路航)

CAS Key Laboratory of Mechanical Behavior and Design of Materials, Department of Modern Mechanics, University of Science and Technology of China (USTC), Hefei, Anhui, China

Wanquan Jiang (江万权)

Department of Chemistry, University of Science and Technology of China, Hefei, Anhui, China

(Received 10 October 2011; final revision received 21 June 2012; published 2 August 2012)

Synopsis

To fully understand the structure dependent mechanical property, the harmonic strain loadings were applied to the magnetorheological plastomer (MRP) to study their dynamic properties. Under different test conditions, nonlinearity which was induced by strain amplitude and driving frequency was generated. In order to investigate the mechanism of nonlinearity, a facile and effective strategy by analyzing the response stress and actuating strain within an oscillatory cycle was introduced. In addition, the microstructures of isotropic and anisotropic MRP were observed and the time dependence of dynamic properties for MRP (from isotropic to anisotropic) under an 800 mT magnetic field was also investigated, which were helpful to further understand the structure dependent dynamic properties depending on actuating strain amplitude. © *2012 The Society of Rheology*. [http://dx.doi.org/10.1122/1.4739263]

I. INTRODUCTION

Dynamic properties, including storage modulus, loss modulus, and loss factor, are important characteristics for viscoelastic materials. Within the linear viscoelastic (LVE) range, the response stress of viscoelastic materials for a sinusoidal strain loading is also sinusoidal. Above the LVE range [nonlinear viscoelastic (NLVE) range] high order harmonics are appeared, which indicates that the stress is nonlinearly dependent on the strain amplitude [McKinley *et al*. (2008)]. The dynamic properties change a lot when it transforms from the LVE to the NLVE range and the physical interpretation of dynamic properties is no longer the same as the ones in the LVE range because of the generation of nonlinear response stress [Ahn *et al*. (2005); Petekidis and Carrier (2009); Wang *et al*. (2009)]. Thus, the study on the

[a]Author to whom correspondence should be addressed. Fax: +86 551 3600419. Electronic mail: gongxl@ustc.edu.cn
[b]Electronic mail: xuansh@ustc.edu.cn

LVE range has drawn many attentions to fully understand the rheological phenomenon and the microcosmic mechanism of the viscoelastic materials.

Large amplitude oscillatory shear (LAOS) is a most used method to determine the transition point between LVE and NLVE ranges. Within the LVE range, the storage modulus of viscoelastic materials is independent on the strain while above LVE range the storage modulus will decrease pronouncedly with the increasing of strain amplitude [Hough *et al*. (2004); Kobelev and Schweizer (2005); Tong *et al*. (2011)]. With this criterion, the LVE range can be easily obtained. Analyzing the shape of strain-stress hysteresis loop (which is also called Lissajous curve) within an oscillatory cycle is another facile and effective strategy to determine the LVE range [McKinley *et al*. (2008); Ng *et al*. (2011); Petekidis *et al*. (2010); Wang *et al*. (2009)]. If the actuating strain is fell in the LVE range of viscoelastic material under a specific oscillatory test condition, the hysteresis loop drawn by sinusoidal actuating strain and response stress is elliptical in shape, or else a nonelliptical plot will be generated due to the appearance of high order harmonics in response stress. In addition, stress-strain curves under rotational shear testing can also be used for the judgment of LVE range [Ihlemann and Besdo (2003); Li *et al*. (2010); Lubarda *et al*. (2003); McKinley and Ng (2008)].

Magnetorheological (MR) materials, including MR fluids [Bossis and Lemaire (1991); de Vicente *et al*. (2011); Lemaire *et al*. (1995); Li *et al*. (2001); Park *et al*. (2010)], MR elastomers [Bellan and Bossis (2002); Boczkowska and Awietjan (2009); Chen *et al*. (2007); Ginder *et al*. (1999); Gong *et al*. (2005); Hu *et al*. (2005); Wei *et al*. (2010a)], and MR gels [An *et al*. (2010); Fuchs *et al*. (2005); Fuchs *et al*. (2004); Hu *et al*. (2006); Mitsumata and Abe (2009); Mitsumata and Ohori (2011); Mitsumata *et al*. (2006); Mitsumata *et al*. (2008); Negami and Mitsumata (2011); Park *et al*. (2011); Shiga *et al*. (1995); Wei *et al*. (2010b); Wilson *et al*. (2002); Wu *et al*. (2011)], are typical viscoelastic materials with controllable rheological properties under an external magnetic field. Many attempts have been made to investigate the viscoelasticity of MR materials. Li *et al*. (1999, 2003) and Claracq *et al*. (2004) studied the nonlinear viscoelasticity of MR fluids under LAOS and rotational tests and further pointed out that the nonlinearity originates from the variation of microstructure. The stress-strain hysteresis loops of MR elastomers under different magnetic field, strain amplitude, and driving frequency within an oscillatory cycle and stress-strain curves under rotational shear testing were also investigated by Li *et al*. (2010). Kaleta and Lewandowski (2007), Kaleta *et al*. (2007), and Zajac *et al*. (2010) prepared two kinds of MR composites by injecting MR fluids into a porous matrix and dispersing micrometer sized iron powder into a thermoplastic matrix, tested the stress-strain hysteresis loops, and explained the physical meaning of experimental results. Due to their special magnetic dependent viscoelastic characteristic, the study of the nonlinearity of MR materials is of great interest not only for their potential applications under various loadings but also for the relationship between microstructure evolution and viscoelasticity will be useful for explaining the MR mechanism.

A kind of solid-like MR gels has recently attracted increasing attentions. In comparison to the conventional MR fluids, the MR gels display a solid-like structure and no particle sedimentation exists. An *et al*. (2010) prepared a highly swollen physical gel by dispersing ferromagnetic particles into triblock copolymers with a high MR effect and stable microstructure. Mitsumata and Ohori (2011) reported a new MR elastomer consists of polyurethane and carbonyl iron particles, the iron particles in this new MR elastomer are moveable. Very recently, a poly (vinyl alcohol) (PVA) hydrogel containing carbonyl iron particles was prepared by Wu *et al*. (2011), a stable chain-like microstructure of this hydrogel can be kept even removing external magnetic field. Different from the MR elastomer, the particles in the MR gels can be rearranged by applying an external magnetic

field. The rearrangement of particles will change the rheological performance, which will be useful in studying their magnetic dependent mechanic property. It is well known that the LVE range is highly affected by the microstructure; thus, the study on the nonlinear viscoelasticity of MR gels is critical to the formation mechanism of the magnetorheological effects. However, the nonlinear viscoelasticity of MR gels has not been systematically investigated.

Recently, our group has reported a plasticine-like MR material which was prepared by mixing carbonyl iron particles with a kind of plastic polyurethane matrix. Due to their plastic properties at room temperature, this kind of MR material was named as MR plastomer (MRP). Except for high MR effect, the iron particles in this material can align parallel to the direction of external magnetic field and keep their locations after removing the external magnetic field. For their special structural characteristic, the MRP is expected to be an ideal candidate for investigating the MR mechanism. In this work, the harmonic strain loadings were applied to MRP to study their dynamic properties. The influences of strain amplitude, driving frequency, and magnetic field on the dynamic properties of MRP were discussed. Three methods were used to determine the LVE range and the reasons for the generation of nonlinearity caused by strain amplitude and driving frequency were explained, respectively. In addition, the microstructures of isotropic MRP and anisotropic MRP were observed as well as the formation mechanism was discussed.

II. EXPERIMENTAL

A. Fabrication of MRP

The MRP was prepared by mixing carbonyl iron particles (type CN, provided by BASF in Germany with an average radius of 6 μm) with a plastic polyurethane matrix, which was synthesized by a chemical method. At first, toluene diisocyanate (TDI, 2,4 - $\approx$ 80%, 2,6 - $\approx$ 20%, Tokyo Chemical Industry Co., Ltd., Japan) and polypropylene glycol [PPG-1000, Mn = 1000, Sigma-Aldrich (Shanghai) Trading Co., Ltd., China] were mixed in a 250 ml three necked round bottom flask with a molar ratio of 3:1. The reaction temperature at this stage was set as 75 °C and this reaction stage lasted about 2 h. After that, 1, 4-butanediol (BDO, Sinopharm Chemical Reagent Co., Ltd., China) that was selected as chain extender was added into reactor at 65 °C, the weight of BDO can be calculated by the following formula:

$$m_{\mathrm{BDO}} = 90.12\mathrm{g\ mol^{-1}} \times \left(\frac{m_{\mathrm{TDI}}}{174.15\mathrm{g\ mol^{-1}} \times 1.1} - \frac{m_{\mathrm{PPG}}}{1000\mathrm{g\ mol^{-1}}} \right), \tag{1}$$

where m_{TDI}, m_{PPG}, and m_{BDO} represent the weight of TDI, PPG, and BDO, respectively. This stage can be named as chain-extending reaction. One hour later, the temperature of reaction system was reduced to 60 °C and then the catalyst stannous octoate (Sinopharm Chemical Reagent Co., Ltd., China) about 0.15 g was added into the flask. The reaction finished when the viscosity of reactants increased obviously after the catalyst stannous octoate (Sinopharm Chemical Reagent Co., Ltd., China) (about 0.15 g) was added into the flask. It is worth noting that the reactants were agitated by stirrer during the whole process and moderate acetone (Sinopharm Chemical Reagent Co., Ltd., China) was added to avoid gelation. Finally, the iron particles with 70% weight fraction were added into the matrix before it cooled down. The mixture was stirred vigorously for a long enough time until the matrix and iron particles were well mixed. In the synthesis process, no magnetic field was applied to the mixture, so the freshly prepared MRP was isotropic.

Before testing, the product was placed at room temperature for at least a week until the performance of the product was stable (it was found that the rheological properties of MRP will trend to stable a week later).

B. Microstructure characterization and MR measurements

An environmental scanning electron microscope (SEM, Philips of Holland, model XT30 ESEM-MP) with an accelerating voltage of 20 kV was used to observe the microstructures of MRP products. Both MRP products in the absence and the presence of magnetic field were placed into liquid nitrogen until they were frozen into pieces, proper cross sections were chosen for observation.

The rheological properties of MRP products were measured by a parallel-plate rheometer (Physica MCR 301, Anton Paar Co., Austria). In addition, an accessory named MRD 180 was configured to make sure the MR properties of MR materials can be measured. The power supply unit PS-DC/MRD is required to control the magnetic field in the MRD 180. The unit is connected to the analog output connectors of the instrument, with which a magnetic flux density range of 0–930 mT can be achieved by adjusting the coil current from 0 A to 4 A. The MRP sample is placed between two parallel plates (the type of rotor: PP20/MRD, SN10036) and the gap of parallel plates was set as 1 mm. The diameter of MRP sample was 20 mm while its thickness was prepared as 1 mm accordingly.

For oscillatory tests, a sinusoidal strain loading was applied to the sample by the rotating plate. The response signals were collected by the torque sensor and processed by the RHEOPLUS software. The parameters of dynamic properties such as storage modulus (G'), loss modulus (G''), and loss factor ($\tan\delta$) can be read from the RHEOPLUS software. However, from the RHEOPLUS software, it is difficult to get the raw signals which may be more informative. For this reason, a plug-in named Rheoplus LAOS module was developed by Anton Paar Co. With this plug-in, the raw signals, including strain and stress waveform with 257 sampling points for each measuring point under dynamic testing can be recorded and analyzed. Stress-strain hysteresis loop can be constructed by strain and stress waveform within an oscillation cycle. Except for the parameters of dynamic properties and energy relationship which can be calculated easily from the stress-strain hysteresis loop, it is easy to determine that whether the materials is LVE under a specific testing condition or not by observing the shape of stress-strain hysteresis loop. This is important because it is controversial to judge the LVE range and difficult to make sure the rationality of the test results. More details will be introduced in Sec. III.

Due to the limitation of the instrument, the experiment results will deviate from the setting value. For example, when the actuating strain amplitude was fixed as 0.2%, the resulting strain amplitude will be a little different from the fixed value. Fortunately, this deviation has nearly no influence on the questions those we focus on. The discrepancy between experimental results and the setting values can be found from the relevant figures in Sec. III. We can only diminish the difference as much as possible to make sure that the experimental results do not deviate from the setting value too much.

III. RESULTS AND DISCUSSION

A. Microstructures of MRP and its time-dependent properties under magnetic field

Figure 1 shows the microstructures of MRP products without and with applying external magnetic field. A homogeneous distribution of iron particles for the freshly prepared MRP can be observed in Fig. 1(a), so the MRP product in this state can be named as

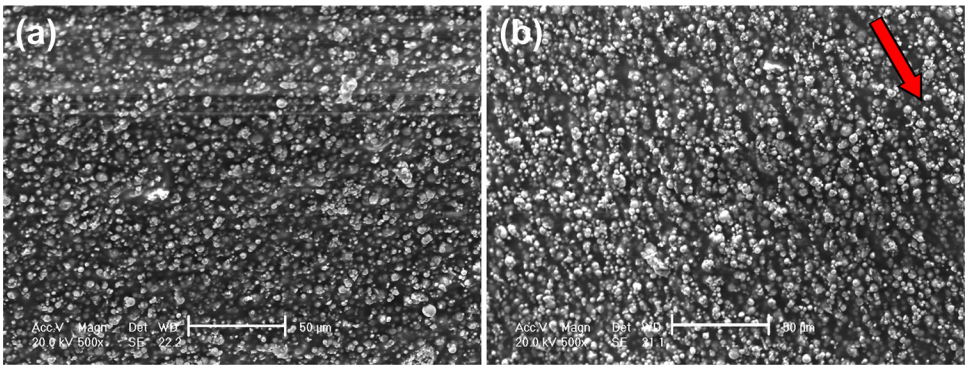

FIG. 1. SEM images of MRP with different processing method: (a) The freshly prepared MRP without magnetic field; (b) the freshly prepared MRP with a magnetic field of 800 mT applied for 10 min. The scale bar on the images corresponds to 50 μm and the red arrow represents the direction of applied magnetic field.

isotropic MRP. If an 800 mT magnetic field is applied to the isotropic MRP for 10 min (this process is similar with the preconfiguration of MR elastomers), the iron particles will move aligned parallel to the direction of magnetic field and form chain-like structures [Fig. 1(b)]. Our previous work proved that these chain-like structures are stable if the magnetic field direction is parallel with the iron particle chains [Xu *et al.* (2011)]. This MRP product with chain-like structures is defined as anisotropic MRP. Strictly speaking, this kind of MRP product can be regarded as transversely isotropic material because the cross section perpendicular to the iron particle chains is isotropic. (The following mentioned MRP represents the anisotropic MRP unless a special explanation is given.) It can be concluded that magnetic field has an important influence on distribution of iron particles in the MRP product. Further, the distribution of iron particles will affect the dynamic rheological properties of MRP.

The changes of G' and $\tan\delta$ of isotropic MRP with time under an external magnetic field of 800 mT are shown in Fig. 2. (In fact, Fig. 2 illustrates the preconfiguration process of MRP.) G' shows an increasing tendency with time at first and then trends to level off after 5 min. At the same time, a remarkable descent of $\tan\delta$ is observed at the first

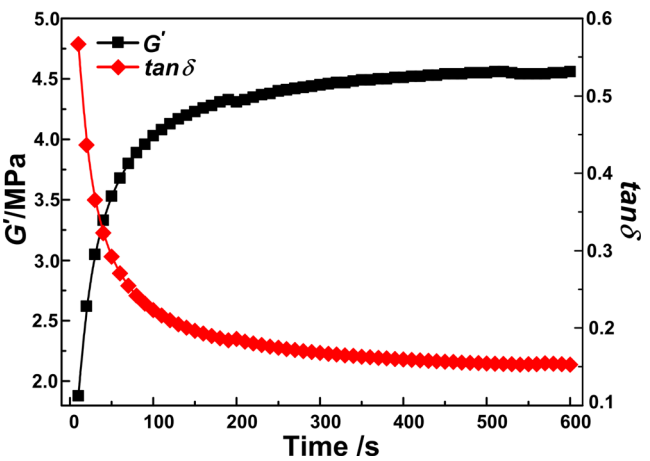

FIG. 2. Dynamic properties of isotropic MRP changed with time under an external magnetic field of 800 mT (the strain amplitude was set as 0.2% while the driving frequency was 5 Hz).

5 min. In fact, the microstructures of MRP under different preconfiguration time (0, 5, and 10 min) were observed; the preconfiguration time for 0 and 10 min is represented in Fig. 1. Therefore, it is obvious that the change of macroscopical mechanical properties is relevant to the evolution of iron particles distribution in the isotropic MRP under external magnetic field. Conversely, the dynamic properties are insensitive to time after 5 min, indicating that the microstructure is stable under the fixed testing conditions (the strain amplitude was set as 0.2% while the driving frequency was 5 Hz). One of the evidence is that no difference between the microstructures of MRP with preconfiguration time of 5 and 10 min (the microstructures with preconfiguration time of 5 min are not shown here) can be observed. In addition, the same microstructures of MRP with preconfiguration time of 5 and 10 min suggest that the anisotropic MRP is generated after applying a magnetic field of 800 mT for 5 min.

B. Strain amplitude sweep and the determination of LVE range

The strain amplitude dependence of G', G'', and $\tan\delta$ for MRP under different magnetic field was investigated. The dynamic rheological performance of MRP without magnetic field is quite different from that of MRP with magnetic field [Figs. 3(a)–3(c)]. G' of MRP without magnetic field decreases slightly with the increasing of strain amplitude. For the case of applying an external magnetic field to MRP, if the strain is smaller than 0.1% G' of MRP almost keeps constant. However, the G' of MRP decreases sharply with the increasing of strain when strain exceeds 0.1%; this phenomenon was also found in MRF and MRG [Claracq *et al*. (2004); Hu *et al*. (2006); Li *et al*. (2003); Mitsumata *et al*. (2008); Wei *et al*. (2010b)] and was called as the Payne effect. The Payne effect may be

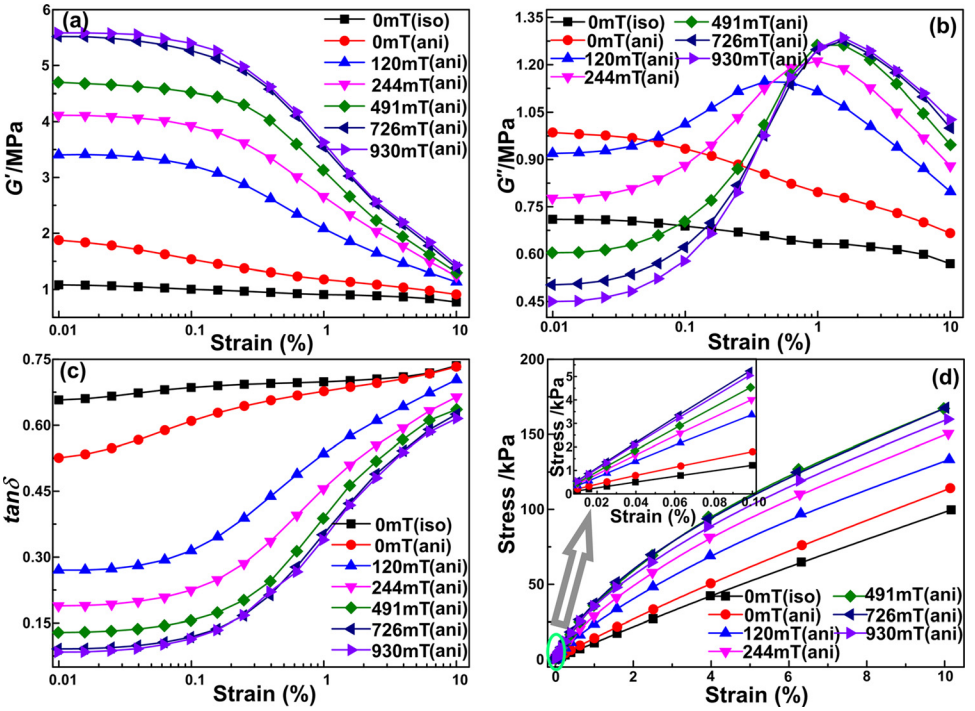

FIG. 3. Dynamic properties (a, b, and c) under oscillatory shear rheometry (the driving frequency was set as 5 Hz) and stress-strain relationship (d) under rotational shear rheometry with different strain amplitude and magnetic field. The "iso" after the legend represents isotropic MRP while the "ani" represents anisotropic MRP.

caused by the destruction of particle chains under a large amplitude strain. In this case, a critical strain γ_c is defined to distinguish the destructive transition point of microstructures of viscoelastic materials [Claracq *et al*. (2004)]. If the strain is smaller than the critical value, the material is stable and its microstructure has not been destroyed, the range from zero to γ_c is defined as LVE range. Correspondently, the range of strain which exceeds γ_c is named as NLVE range. With this criterion, the LVE range of MRP with magnetic field is 0–0.1% and the MRP without magnetic field has no apparent NLVE range if the strain amplitude keeps below 10% (Fig. 3).

Another method to determine LVE range is analyzing the relationship between the response stress and actuating strain within an oscillatory cycle [Lakes (2009)]. If a sinusoidal strain loading is applied to the LVE material, the response stress is also a sinusoidal function with the same angular frequency and a phase shift. The mathematic formula can be expressed as follows:

$$\begin{cases} \gamma = \gamma_0 \sin \omega t, \\ \tau = \tau_0 \sin(\omega t + \delta) = G\gamma + \eta \dfrac{d\gamma}{dt} = G\gamma_0 \sin \omega t + \eta \gamma_0 \omega \cos \omega t, \end{cases} \tag{2}$$

where the first item at the right of the stress equation represents the elastic component and the second item indicates the viscous component. For NLVE material, the response stress to a sinusoidal strain loading will be expressed by a Fouier series of odd harmonics [Li *et al*., 2003)], which means that higher harmonics of driving frequency generate due to the nonlinearity of the viscoelastic material:

$$\begin{cases} \gamma = \gamma_0 \sin \omega t, \\ \tau = \displaystyle\sum_{n=1,\text{odd}}^{N} \tau_n \sin(n\omega t + \delta_n). \end{cases} \tag{3}$$

If we eliminate the intermediate parameter t, the response of material to sinusoidal loading can be visualized by a plot of strain vs stress. According to Eqs. (2) and (3), it can be concluded that the stress-strain plot for LVE material under sinusoidal loading is elliptical while NLVE material will give rise to a nonelliptic stress-strain plot because of harmonic distortion. Further, the proportion of high order harmonics in the first order harmonic can be quantified by Fourier transform (FT) rheology [Wang *et al*. (2009); Wilhelm *et al*. (1999)].

In this work, the stress-strain plots of MRP under different strain amplitude in a cycle period were measured (Fig. 4). It is obvious that the stress-strain plots of MRP without magnetic field can form nice elliptical shapes when strain amplitudes ranged from 0 to 10% are applied [Figs. 4(b), 4(d), and 4(f)], which demonstrates that the MRP without magnetic field can be treated as LVE material within the strain amplitude range of 0–10%. This result is consistent with the conclusion made by the LAOS. However, the stress-strain plots of MRP with magnetic field of 491 mT are also nice elliptical shapes if strain amplitudes are less than 1% [Figs. 4(a) and 4(c)]. In comparison to the LVE range obtained by the LAOS (0.1%), this value is higher. Within the LVE range of 0–0.1%, a tiny strain excitation which does not change the microstructure of material will get a linear stress response. In the previous reports, it was believed that once the microstructure was destroyed, the nonlinearity begins [Li *et al*. (2003); Mitsumata *et al*. (2008); Wang *et al*. (2009)]. However, based on the above analysis, it can be concluded that the MRP material can still keep linearity if the microstructure is only partly destroyed even though

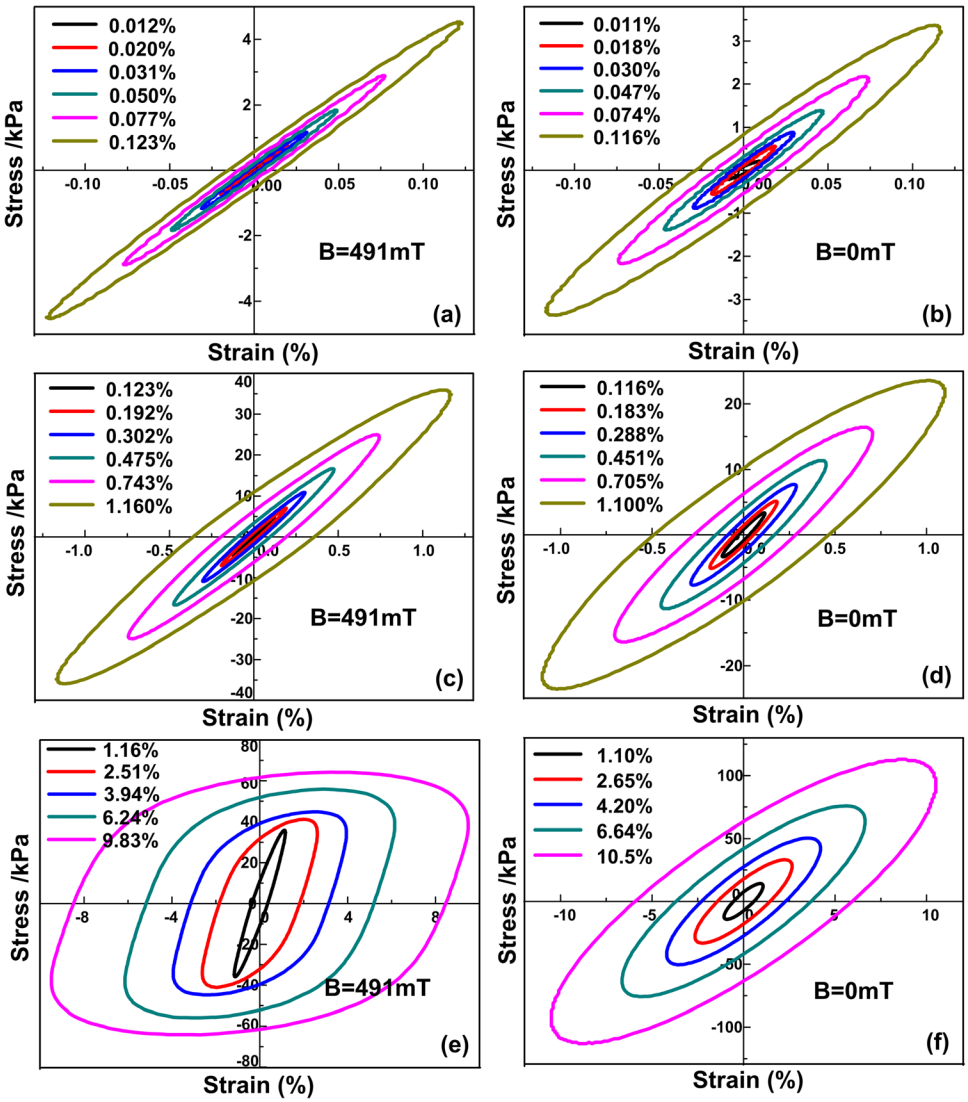

FIG. 4. Stress-strain plots of MRP with (a, c, and e in the strain amplitude range of 0–0.1%, 0.1%–1%, and 1–10%, respectively) and without (b, d, and f in the strain amplitude range of 0–0.1%, 0.1%–1%, and 1%–10%, respectively) magnetic field at different strain amplitude. The values after the legend represent the maximum of strain for each hysteresis loops.

the destruction of microstructure has great influence on the dynamic performance of MRP [Figs. 3(a)–3(c)]. If a sinusoidal strain with amplitude ranged from 1.16% to 9.5% is applied to MRP, the shapes of stress-strain plots will not be elliptical [Fig. 4(e)], which indicates that nonlinearity of MRP generates and this nonlinearity is caused by destruction of microstructure under a large enough strain amplitude. In addition, the definition of dynamic property parameters based on LVE theory will make no sense when applied strain amplitude exceeds 1%.

Based on the hysteresis loops shown in Fig. 4, the dynamic properties can be further calculated. For elliptical hysteresis loops [as shown in Figs. 4(a)–4(d) and 4(f)], the relationship between the geometry of stress-strain plot and dynamic properties is shown in

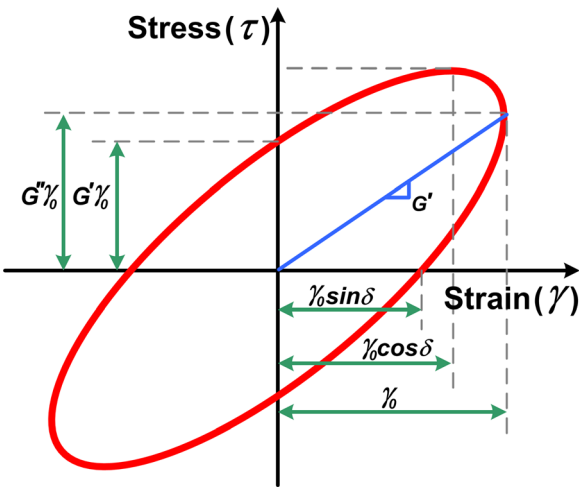

FIG. 5. Stress-strain plot for linear viscoelastic material under sinusoidal actuating loading and the relationship between geometry and dynamic properties.

Fig. 5 according to LVE theory [Lakes (2009)]. G' can be obtained by calculating the slope of the line from the origin to the point of maximum strain. G'' is relevant to the energy dissipation per volume within an oscillatory cycle. To find the dissipated energy, consider the strain and stress represented by Eq. (2) and integrate over a full cycle:

$$\begin{aligned} W_d &= \int_0^{2\pi/\omega} \tau \frac{d\gamma}{dt} dt \\ &= \tau_0 \gamma_0 \omega \int_0^{2\pi/\omega} [\cos \omega t \sin \omega t \cos \delta + \cos^2 \omega t \sin \delta] dt \\ &= \pi \tau_0 \gamma_0 \sin \delta = \pi G'' \gamma_0^2. \end{aligned} \tag{4}$$

The dissipated energy density W_d can also be calculated by the area within the hysteresis loop, and then, G'' can be calculated by Eq. (4). If the hysteresis loop is no longer elliptical in shape, the LVE model [Eq. (2)] is not suitable for describing the rheological behaviors of MRP. For the classical NLVE model [Eq. (3)], the high order items have no explicit physical meanings, which have little help to further understand the complex nonlinear behaviors. In this study, an equivalent method was introduced when it comes to Fig. 4(e). An equivalent storage modulus G'_{equ} can be defined by calculating the slope of the line from the origin to the point of maximum strain. In the same way, an equivalent loss modulus G''_{equ} can also be calculated by Eq. (4). It needs to be emphasized that although defined in the similar way based on hysteresis loop, the physical meaning of dynamic properties defined here is not the same as the situation in LVE material [Ahn *et al.* (2005)]. However, in comparison to the classical NLVE model [Eq. (3)], this equivalent method avoids discussing the high order items which have no explicit physical meanings. The equivalent dynamic properties are valuable to some extent in characterizing the stiffness and the energy dissipation of MRP under LAOS.

Figure 6(a) shows dissipated energy density W_d of MRP per oscillatory cycle with and without magnetic field at different strain amplitude. The values of W_d are the areas of hysteresis loops shown in Fig. 4. It is obvious that W_d increases with the increasing of the strain amplitude. Interestingly, the W_d of MRP without magnetic field is larger than that

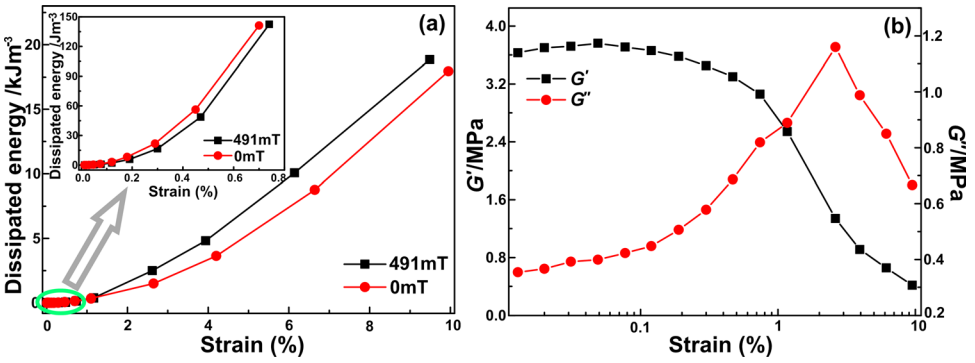

FIG. 6. Dissipated energy per cycle of MRP with and without magnetic field (a) and dynamic properties calculated by stress-strain plots of MRP with an external magnetic field of 491 mT (b) at different strain amplitude (the driving frequency was set as 5 Hz).

of MRP with magnetic field if strain amplitude is lower than 1% [the inset of Fig. 6(a)]. Contrastingly, the W_d of MRP with magnetic field is larger than that of MRP without magnetic field when strain amplitude exceeds 1% [Fig. 6(a)]. As we know, the energy dissipation comes from interfacial slipping and the damping of matrix is caused by the movement of soft segment in polyurethane (the damping of iron particles can be ignored compared with that of matrix) [Xu *et al.* (2011)]. At a small strain, the microstructure of MRP cannot be destroyed, the interfacial slipping between iron particles and matrix can be ignored. At the same time, the magnetic interactions between iron particles will prevent the movement of soft matrix, which causes a smaller energy dissipation of MRP with magnetic field. With the increasing of the strain amplitude, the iron particle chains are deflected along the direction of strain more and more obviously. The magnetic interactions between iron particles induced by an external magnetic field will impel the iron particles to move to their initial positions. As a result, considerable energy dissipation will be caused by interfacial slipping due to the iron particles movement. This additional energy dissipation caused by external magnetic field will make W_d of MRP with magnetic field be larger than that of MRP without magnetic field at large strain amplitude.

The strain amplitude dependence of G' and G'' calculated by the hysteresis loops of MRP with magnetic field [Figs. 4(a), 4(c), and 4(e)] and dissipated energy [Fig. 6(a)], respectively, is shown in Fig. 6(b). The calculation results have the same tendency with the experimental results [Figs. 3(a) and 3(b)], indicating that the calculation results are reasonable to some extent. From the fact that G' calculated by the hysteresis loops decreases with the increasing of the strain amplitude and G'' increases with the increasing of the strain amplitude in the range of 0.1%–1%, it can also be concluded that the dynamic properties are very sensitive to the microstructure destruction of MRP. But the judgment of linear viscoelasticity for MRP cannot be only determined by the change of dynamic properties according to the above analysis. It is need to note that the differences between the experimentally obtained results [Figs. 3(a) and 3(b)] and the results calculated by the hysteresis loops (Fig. 4) are ascribed to the different equivalent method. It is well known that the strain under rotational shear mode is heterogeneous (the strain at edge of sample is largest while the strain at the center of sample is equal to zero). An equivalent strain is used in rheometer. However, the computing formula for the equivalent strain and other dynamic parameters in the RHEOPLUS software is unknown, so it is difficult to discuss the reason for the discrepancy between experimental results and computing results in value. But from the same tendency in Figs. 3(a), 3(b), and 6(b), it can be

deduced that both of the results are relevant with the hysteresis loops (in other words, the experimental results are proportional to the computing results), and this is what we are concerned.

The quasistatic shear behavior of MRP was also investigated. Figure 3(d) shows the stress-strain curves of MRP under different magnetic field by rotational shearing. The shear modulus can be obtained by identifying the tangent of the specific plot on stress-strain curves. The stress-strain relationship of MRP in the range of 0–0.1% is shown in the inset of Fig. 3(d), from which it can be found that the shear moduli of MRP under different magnetic field are constant because of the linear relationship between stress and strain. Within the strain amplitude of 10%, the shear modulus of MRP without magnetic field keeps constant while the shear modulus of MRP decreases with the increasing of strain amplitude when an external magnetic field is applied. Decreasing of shear modulus means nonlinearity appears in MRP. Nevertheless, it can still be found from Fig. 3(d) that the shear modulus of MRP under an external magnetic field is approximatively constant if strain amplitude is in the range of 0.1%–1%. In sum, a linear stress-strain behavior of MRP under an external magnetic field was found when applied strain amplitude does not exceed 1% according to the quasistatic rotational shearing results, which is consistent with the results obtained by oscillatory shear rheometry.

Furthermore, it can also be found from Fig. 3 that the isotropic MRP and anisotropic MRP show different rheological performance without magnetic field, indicating that iron particle distribution has significant influence on the rheological performance of MRP. As shown in Figs. 3(a) and 3(c), G' of anisotropic MRP is larger than that of isotropic MRP while $\tan\delta$ of anisotropic MRP is smaller than that of isotropic MRP. This result also origins from microstructure discrepancy of MRP (see Fig. 1). The MRP with ordered microstructure [Fig. 1(b)] will lead up to large restriction effect on external driving force and the movement of soft chain segments in the matrix in comparison to the MRP with disordered microstructure [Fig. 1(a)], which induces larger G' and smaller $\tan\delta$.

C. Frequency sweep and the nonlinearity induced by driving frequency

Except for strain amplitude, driving frequency is another important influence factor on dynamic rheological performance of MRP. At fixed strain amplitude of 0.1%, the frequency sweep mode was applied to MRP and the frequency was swept from 1 Hz to 100 Hz. The frequency dependence of G' and $\tan\delta$ under different magnetic field is shown in Figs. 7(a) and 7(b), respectively. It can be found from Fig. 7(a) that G' exhibits

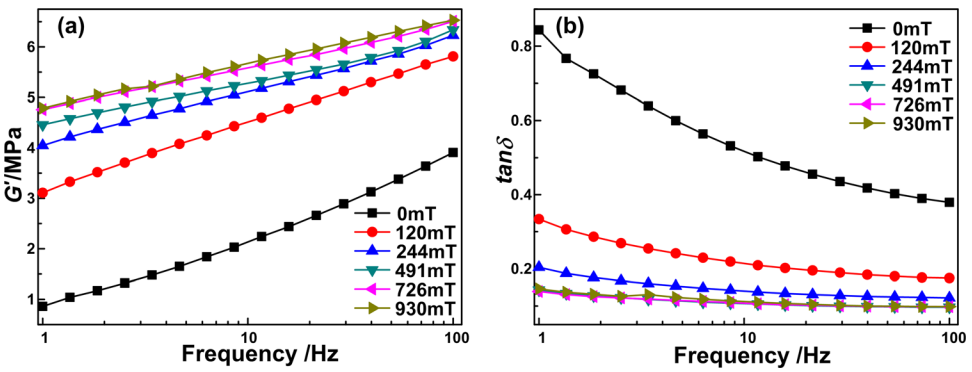

FIG. 7. Storage moduli (a) and loss factors (b) by oscillatory tests under different driving frequency and magnetic field (the actuating strain amplitude was set as 0.1%).

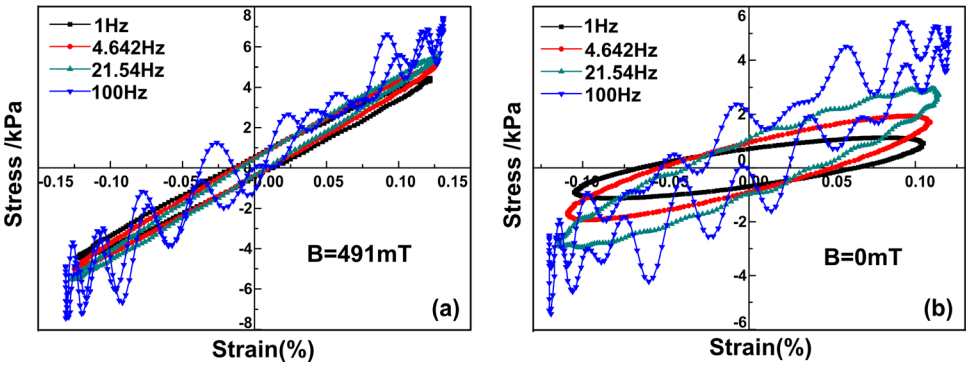

FIG. 8. Stress-strain plots of MRP with (a) and without (b) magnetic field at different driving frequency.

an increasing tendency with frequency and a linear relationship with logarithm of frequency. At the same time, $\tan\delta$ decreases gradually with increasing of the frequency. However, as magnetic field is increased, the tendency that $\tan\delta$ decreases with frequency becomes more and more slightly [Fig. 7(b)]. Different from strain amplitude sweep, it cannot find a critical frequency from which the dynamic properties of MRP will change dramatically, which means that it is difficult to determine whether a frequency-induced nonlinearity will generate in the range of 1–100 Hz from Fig. 7.

The raw data of stress-strain plots for every point in Fig. 7 can be obtained by using Rheoplus LAOS module when frequency sweeping was applied to MRP. The stress-strain hysteresis loops of MRP with and without magnetic field at specified driving frequency are illustrated in Fig. 8. It is easy to determine the linear viscoelasticity by judging whether the hysteresis loop is ellipse or not. It can be seen from Fig. 8 that the stress-strain hysteresis loops with the driving frequency of 1 and 4.642 Hz are all perfect ellipses. When the driving frequency increases to 21.54 Hz, a distortion generates. With further increasing of the frequency, the shape of stress-strain hysteresis loops becomes more and more irregular, just like the shape of stress-strain hysteresis loop at the driving frequency of 100 Hz as shown in Fig. 8. In fact, the stress-strain plots at the driving frequency lower than 20 Hz are all elliptical in shape and the stress-strain plots with the driving frequency from 21.54 to100 Hz are all irregular (data is not shown). This shape changing of stress-strain hysteresis loops reveals that the driving frequency can induce nonlinearity of MRP as well. In addition, the same laws are observed in Figs. 8(a) and 8(b), indicating that the magnetic field has no influence on the frequency-induced nonlinearity.

Dynamic properties do not change dramatically with the frequency being swept from 1 to 100 Hz, indicating that the microstructure of MRP is not destroyed by large driving frequency. Therefore, the reason for the generation of frequency-induced nonlinearity is not the same as the one of the strain amplitude-induced nonlinearity. Wall slip effect is one of the possible reasons and this possibility can be excluded by the following analysis. First, the MRP itself is a kind of good adhesive, which makes MRP combine well with the plates of rheometer. In particular, it is more difficult to remove the upper plate from MRP under magnetic field than that in the absence of magnetic field, indicating that the magnetic force is helpful to improve the combination between MRP and plates. Second, a strain amplitude sweep test at the frequency of 100 Hz under different magnetic field strength was performed (data are not shown). A sharp decrease of G' can be found when actuating strain exceeds 1%, which is the most different part in comparison with

Fig. 3(a). This sharp decrease may be caused by wall slip, indicating that the slipping between MRP and plates will happen at large actuating strain and high driving frequency (in other words, the wall slip effect will not happen at small actuating strain, just like the situation in Fig. 8 at a actuating strain of 0.1%). Third, as far as we know, the wall slip effect is relevant with the kinetic friction between the plate and the surface of sample, so the response stress is relevant with the relative slipping velocity between the plate and the surface of sample. If a sinusoidal actuating strain is applied to the sample, the largest strain rate will generate at the position where the strain is equal to zero. Large strain rate, which indicates large relative slipping velocity, will result in large kinetic friction. In other words, if the response stress is caused by wall slip effect, the large response stress will appear at the position where the strain is small. In addition, the strain rate changes with sinusoidal strain smoothly, indicating that the wall slip-induced response stress will change with the strain continuously. However, as shown in Fig. 8, the largest strain appears at the position where the stain is largest and the stress-strain plots distort with many small wave crests. These results are quite different from the condition that caused by wall slip effect.

Another reason for frequency-induced nonlinearity is inertia of MRP generating at high frequency. A schematic diagram that illustrates an actuating torque is applied to viscoelastic material and a response signal is collected by a torque sensor by oscillatory shearing (Fig. 9). In this work, the MRP sample is considered in the oscillatory shear system separately, an equilibrium equation can be presented as follows [Lakes (2009)]:

$$M_{\text{ext}} - M_{\text{res}} = I\frac{d^2\theta}{dt^2}, \tag{5}$$

where $M_{\text{ext}} = M_0 e^{i\omega t}$ is the external torque applied to MRP with angular frequency of ω, M_{res} is the response torque which involves the information about MRP, I is the moment of inertia of MRP, and $\theta = \theta_0 e^{i\omega t}$ is the torsion angle in phase with external torque.

At low frequency, the inertia item $I\frac{d^2\theta}{dt^2} = -I\omega^2\theta_0 e^{i\omega t}$ can be neglected compared with the external torque. As a result, the frequency-induced nonlinearity that is mainly induced by the inertia item can also be neglected. As the driving frequency increases to 21.54 Hz, the inertia item has to be taken into account because it is proportional to the square of angular frequency. Then, a nonlinear item with square of angular frequency is introduced into the equilibrium equation and the nonlinear results will be generated (Fig. 8). Therefore, the frequency-induced nonlinearity can be well explained by the inertia of MRP at

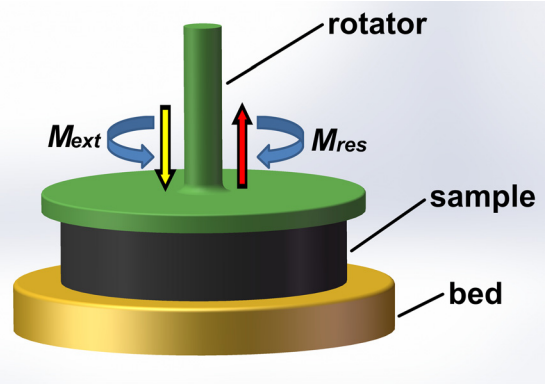

FIG. 9. Schematic diagram of oscillatory shear system with an actuating torque and a response torque signal.

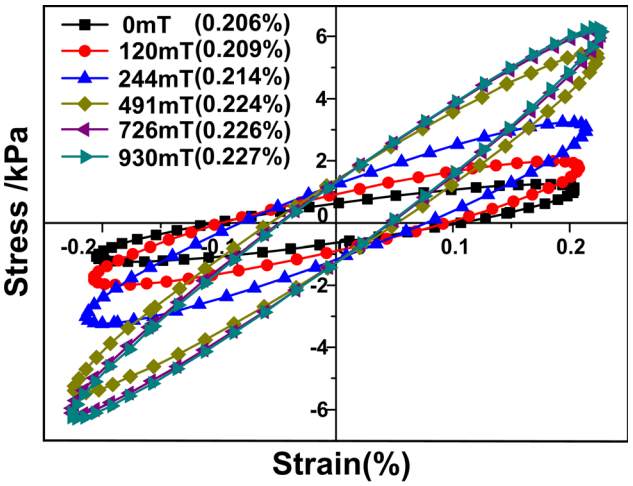

FIG. 10. Stress-strain plots of MRP with different magnetic field at a fixed strain amplitude of 0.2% and a driving frequency of 5 Hz. The values after the legend represent the magnetic field and strain amplitudes, respectively.

high frequency. The frequency-induced nonlinearity should be avoided because the material property will be difficult to be analyzed from the response stress when taking into account the inertia item. For MRP, the oscillatory shear rheometry which is carried out at the frequency lower than 20 Hz will obtain the valid results that can neglect the influence of the frequency-induced nonlinearity.

D. Magnetic field sweep at fixed strain amplitude and driving frequency

It is well known that magnetic field has an important influence on the dynamic properties of MR material [An *et al.* (2010); Chen *et al.* (2007); Ginder *et al.* (1996)]. For MRP, if the strain amplitude and driving frequency are fixed to ensure the validity of the experimental results, the magnetic field dependence on the rheology of MRP can be easily analyzed. Figure 10 shows the stress-strain hysteresis loops of MRP under different magnetic field. The strain amplitude and driving frequency were set as 0.2% and 5 Hz, respectively. The shapes of stress-strain plots are all perfect elliptical, indicating that MRP at the setting strain amplitude and driving frequency is LVE material. The density of magnetic field has nearly no influence on the nonlinearity of MRP, which is coincident with the results illustrated in Fig. 3. The slope of the line from the origin to the point of maximum strain increases with the increasing of the magnetic field, which means that G' of MRP can be controlled by magnetic field. In addition, there is not obvious increment of the slope under high magnetic field (for example, the stress-strain plot under 726 mT almost coincides with the one under 930 mT). This result demonstrates that MRP is a kind of magnetic-sensitive material at low field, which is relative with the magnetization of iron particles in MRP. In general, it is not so easy to achieve a high magnetic field, so the characteristic of magnetic-controllable ability for MRP under low magnetic field is more valuable in practical applications.

IV. CONCLUSION

In this work, the harmonic strain loadings were applied to the MRP to study their dynamic properties. Nonlinearities were generated when executing the strain amplitude

sweep and frequency sweep under oscillatory shear rheometry, and the mechanisms for the generation of nonlinearity were discussed. The reason for nonlinearity induced by strain amplitude is attributed to the destruction of microstructure. Interestingly, the destruction of microstructure will not cause strain-dependent nonlinearity immediately, though the dynamic properties are very sensitive to the alteration of microstructure of MRP. When the strain amplitude exceeds 0.1%, the storage modulus shows a sharply decreasing trend with increasing of the strain amplitude. However, the nonlinearity appears after the strain amplitude is increased to 1%. The inertia item which is proportional to the square of angular frequency will result in frequency-dependent nonlinearity and this nonlinearity can only be found from strain-stress hysteresis loops when the driving frequency is larger than 21.54 Hz. The oscillatory shear tests of MRP which are carried out at the frequency lower than 20 Hz will obtain the valid results that can neglect the influence of the frequency-induced nonlinearity. Magnetic field has an important influence on the dynamic properties of MR material but has nearly no influence on the nonlinearity induced by the strain amplitude and the driving frequency. These analyses are important for understanding the formation mechanism of the MR materials, which can further support valuable parameters during their applications.

ACKNOWLEDGMENTS

Financial supports from the National Natural Science Foundation of China (Grant Nos. 11125210, 11072234, and 11102202), the National Basic Research Program of China (973 Program, Grant No. 2012CB937500), and the Specialized Research Fund for the Doctoral Program of Higher Education of China (Project No. 20093402110010) are gratefully acknowledged.

References

Ahn, K. H., K. S. Cho, K. Hyun, and S. J. Lee, "A geometrical interpretation of large amplitude oscillatory shear response," J. Rheol. **49**, 747–758 (2005).

An, H. N., S. J. Picken, and E. Mendes, "Enhanced hardening of soft self-assembled copolymer gels under homogeneous magnetic fields," Soft Matter **6**, 4497–4503 (2010).

Bellan, C., and G. Bossis, "Field dependence of viscoelastic properties of MR elastomers," Int. J. Mod. Phys. B **16**, 2447–2453 (2002).

Boczkowska, A., and S. F. Awietjan, "Smart composites of urethane elastomers with carbonyl iron," J. Mater. Sci. **44**, 4104–4111 (2009).

Bossis, G., and E. Lemaire, "Yield stresses in magnetic suspensions," J. Rheol. **35**, 1345–1354 (1991).

Chen, L., X. L. Gong, W. Q. Jiang, J. J. Yao, H. X. Deng, and W. H. Li, "Investigation on magnetorheological elastomers based on natural rubber," J. Mater. Sci. **42**, 5483–5489 (2007).

Claracq, J., J. Sarrazin, and J. P. Montfort, "Viscoelastic properties of magnetorheological fluids," Rheol. Acta **43**, 38–49 (2004).

de Vicente, J., D. J. Klingenberg, and R. Hidalgo-Alvarez, "Magnetorheological fluids: A review," Soft Matter **7**, 3701–3710 (2011).

Fuchs, A., B. Hu, F. Gordaninejad, and C. Evrensel, "Synthesis and characterization of magnetorheological polyimide gels," J. Appl. Polym. Sci. **98**, 2402–2413 (2005).

Fuchs, A., M. Xin, F. Gordaninejad, X. J. Wang, G. H. Hitchcock, H. Gecol, C. Evrensel, and G. Korol, "Development and characterization of hydrocarbon polyol polyurethane and silicone magnetorheological polymeric gels," J. Appl. Polym. Sci. **92**, 1176–1182 (2004).

Ginder, J. M., L. C. Davis, and L. D. Elie, "Rheology of magnetorheological fluids: Models and measurements," Int. J. Mod. Phys. B **10**, 3293–3303 (1996).

Ginder, J. M., M. E. Nichols, L. D. Elie, and J. L. Tardiff, "Magnetorheological elastomers: Properties and applications," *Smart Structures and Materials 1999 Conference*, Newport Beach, CA, March 1–4, 1999, Vol. 3675, pp. 131–138.

Gong, X. L., X. Z. Zhang, and P. Q. Zhang, "Fabrication and characterization of isotropic magnetorheological elastomers," Polym. Test **24**, 669–676 (2005).

Hough, L. A., M. F. Islam, P. A. Janmey, and A. G. Yodh, "Viscoelasticity of single wall carbon nanotube suspensions," Phys. Rev. Lett. **93**, 168102 (2004).

Hu, B., A. Fuchs, S. Huseyin, F. Gordaninejad, and C. Evrensel, "Supramolecular magnetorheological polymer gels," J. Appl. Polym. Sci. **100**, 2464–2479 (2006).

Hu, Y., Y. L. Wang, X. L. Gong, X. Q. Gong, X. Z. Zhang, W. Q. Jiang, P. Q. Zhang, and Z. Y. Chen, "New magnetorheological elastomers based on polyurethane/Si-rubber hybrid," Polym. Test **24**, 324–329 (2005).

Ihlemann, J., and D. Besdo, "A phenomenological constitutive model for rubberlike materials and its numerical applications," Int. J. Plast. **19**, 1019–1036 (2003).

Kaleta, J., and D. Lewandowski, "Inelastic properties of magnetorheological composites: I. Fabrication, experimental tests, cyclic shear properties," Smart Mater. Struct. **16**, 1948–1953 (2007).

Kaleta, J., D. Lewandowski, and G. Zietek, "Inelastic properties of magnetorheological composites: II. Model, identification of parameters," Smart Mater. Struct. **16**, 1954–1960 (2007).

Kobelev, V., and K. S. Schweizer, "Nonlinear elasticity and yielding of depletion gels," J. Chem. Phys. **123**, 164902 (2005).

Lakes, R., *Viscoelastic Materials* (Cambridge University Press, New York, 2009).

Lemaire, E., A. Meunier, and G. Bossis, "Influence of the particle-size on the rheology of magnetorheological fluids," J. Rheol. **39**, 1011–1020 (1995).

Li, W. H., G. Chen, and S. H. Yeo, "Viscoelastic properties of MR fluids," Smart Mater. Struct. **8**, 460–468 (1999).

Li, W. H., H. Du, G. Chen, and S. H. Yeo, "Viscoelastic properties of MR fluids under oscillatory shear," *Smart Structures and Materials 2001 Conference*, Newport Beach, CA, March 5–8, 2001, Vol. 4331, pp. 333–342.

Li, W. H., H. J. Du, G. Chen, S. H. Yeo, and N. Q. Guo, "Nonlinear viscoelastic properties of MR fluids under large-amplitude-oscillatory-shear," Rheol. Acta **42**, 280–286 (2003).

Li, W. H., Y. Zhou, and T. F. Tian, "Viscoelastic properties of MR elastomers under harmonic loading," Rheol. Acta **49**, 733–740 (2010).

Lubarda, V. A., D. J. Benson, and M. A. Meyers, "Strain-rate effects in rheological models of inelastic response," Int. J. Plast. **19**, 1097–1118 (2003).

McKinley, G. H., R. H. Ewoldt, and A. E. Hosoi, "New measures for characterizing nonlinear viscoelasticity in large amplitude oscillatory shear," J. Rheol. **52**, 1427–1458 (2008).

McKinley, G. H., and T. S. K. Ng, "Power law gels at finite strains: The nonlinear rheology of gluten gels," J. Rheol. **52**, 417–449 (2008).

Mitsumata, T., K. Sakai, and J. Takimoto, "Giant reduction in dynamic modulus of kappa-carrageenan magnetic gels," J. Phys. Chem. B **110**, 20217–20223 (2006).

Mitsumata, T., and N. Abe, "Magnetic-field sensitive gels with wide modulation of dynamic modulus," Chem. Lett. **38**, 922–923 (2009).

Mitsumata, T., and S. Ohori, "Magnetic polyurethane elastomers with wide range modulation of elasticity," Polym. Chem. **2**, 1063–1067 (2011).

Mitsumata, T., T. Wakabayashi, and T. Okazaki, "Particle dispersibility and giant reduction in dynamic modulus of magnetic gels containing barium ferrite and iron oxide particles," J. Phys. Chem. B **112**, 14132–14139 (2008).

Negami, K., and T. Mitsumata, "Magnetorheological behaviour of magnetic carrageenan gels against shear and compression strains," e-Polymers, 034 (2011).

Ng, T. S. K., G. H. McKinley, and R. H. Ewoldt, "Large amplitude oscillatory shear flow of gluten dough: A model power-law gel," J. Rheol. **55**, 627–654 (2011).

Park, B. O., B. J. Park, M. J. Hato, and H. J. Choi, "Soft magnetic carbonyl iron microsphere dispersed in grease and its rheological characteristics under magnetic field," Colloid Polym. Sci. **289**, 381–386 (2011).

Park, B. J., F. F. Fang, and H. J. Choi, "Magnetorheology: Materials and application," Soft Matter **6**, 5246–5253 (2010).

Petekidis, G., F. Renou, and J. Stellbrink, "Yielding processes in a colloidal glass of soft star-like micelles under large amplitude oscillatory shear (LAOS)," J. Rheol. **54**, 1219–1242 (2010).

Petekidis, G., and V. Carrier, "Nonlinear rheology of colloidal glasses of soft thermosensitive microgel particles," J. Rheol. **53**, 245–273 (2009).

Shiga, T., A. Okada, and T. Kurauchi, "Magnetroviscoelastic behavior of composite gels," J. Appl. Polym. Sci. **58**, 787–792 (1995).

Tong, Z., W. X. Sun, Y. R. Yang, T. Wang, X. X. Liu, and C. Y. Wang, "Large amplitude oscillatory shear rheology for nonlinear viscoelasticity in hectorite suspensions containing poly(ethylene glycol)," Polymer **52**, 1402–1409 (2011).

Wang, S. Q., X. Li, and X. R. Wang, "Nonlinearity in large amplitude oscillatory shear (LAOS) of different viscoelastic materials," J. Rheol. **53**, 1255–1274 (2009).

Wei, B., X. L. Gong, and W. Q. Jiang, "Influence of polyurethane properties on mechanical performances of magnetorheological elastomers," J. Appl. Polym. Sci. **116**, 771–778 (2010a).

Wei, B., X. L. Gong, W. Q. Jiang, L. J. Qin, and Y. C. Fan, "Study on the properties of magnetorheological gel based on polyurethane," J. Appl. Polym. Sci. **118**, 2765–2771 (2010b).

Wilhelm, M., P. Reinheimer, and M. Ortseifer, "High sensitivity Fourier-transform rheology," Rheol. Acta **38**, 349–356 (1999).

Wilson, M. J., A. Fuchs, and F. Gordaninejad, "Development and characterization of magnetorheological polymer gels," J. Appl. Polym. Sci. **84**, 2733–2742 (2002).

Wu, J. K., X. L. Gong, Y. C. Fan, and H. S. Xia, "Physically crosslinked poly(vinyl alcohol) hydrogels with magnetic field controlled modulus," Soft Matter **7**, 6205–6212 (2011).

Xu, Y. G., X. L. Gong, S. H. Xuan, W. Zhang, and Y. C. Fan, "A high-performance magnetorheological material: Preparation, characterization and magnetic-mechanic coupling properties," Soft Matter **7**, 5246–5254 (2011).

Zajac, P., J. Kaleta, D. Lewandowski, and A. Gasperowicz, "Isotropic magnetorheological elastomers with thermoplastic matrices: Structure, damping properties and testing," Smart Mater. Struct. **19**, 045014 (2010).